Atmos. Chem. Phys. Discuss., 10, 10551–10587, 2010
www.atmos-chem-phys-discuss.net/10/10551/2010/

Atmospheric Chemistry and Physics Discussions

This discussion paper is/has been under review for the journal Atmospheric Chemistry and Physics (ACP). Please refer to the corresponding final paper in ACP if available.

Ozone production during the field campaign RISFEX 2003 in the Sea of Japan: analysis of sensitivity and behavior basing on an improved indicator

Z. Q. Wang, B. Qi, B. Yang, and Y. S. Chen

Key Laboratory of Applied Surface and Colloid Chemistry (Shaanxi Normal University), Ministry of Education, School of Chemistry and Materials Science, Xian 710062, China

Received: 2 April 2010 – Accepted: 13 April 2010 – Published: 21 April 2010

Correspondence to: B. Qi (b.qi@163.com)

Published by Copernicus Publications on behalf of the European Geosciences Union.

Abstract

An improved indicator Φ, based on the present indicator $\Theta = \tau_{OH}^{VOC}/\tau_{OH}^{NO_x}$, is developed to determine the sensitivity of ozone production to HC and NO_x in the field campaign RISFEX 2003 (RIShiri Fall EXperiment 2003) made in September 2003 at Rishiri island (45.07° N, 141.12° E, and 35 m a.s.l.) in the sea of Japan. The indicator, defined as a ratio of k_{HC+OH}[HC] to k_{NO_x+OH}[NO_x], has a close correlation with the relative sensitivity ($d\ln P(O_3)/d\ln$[NO] and $P(O_3)/d\ln$[HC]) which can explicitly give the sensitivity of $P(O_3)$ to NO and HC. According to the indicator, four distinctive regimes were obtained in which modeled $P(O_3)$ behaviors differently with HC and NO_x. At $\Phi < 1$, $P(O_3)$ is located in Regime I and is greatly sensitive to both HC with a positive correlation and NO_x with a negative one. In Regime II ($1 < \Phi < 7 \pm 3$), $P(O_3)$ is more sensitive to HC than NO_x, but has a similar relationship to HC and NO_x. $P(O_3)$ is both positively sensitive to HC and NO_x in Regime III ($7 \pm 3 < \Phi < 23 \pm 7$). For a higher Φ in Regime IV, it was found that $P(O_3)$ is greatly sensitive to NO_x but nearly insensitive to HC. During the campaign, 91% (247/271) of $P(O_3)$ data are located in Regime III and IV, illuminating that NO_x is a limiting factor for ozone production. Hence a controlling of NO_x emission can be a more efficient strategy for ozone abatement at the site.

Detailed comparisons between the experimental and modeled $P(O_3)$ were performed in different regimes and the results show basically an agreement between the two methods. However, the model tended to underestimate $P(O_3)$ in Regime II, indicating that an important source of peroxy radicals missed. In Regime IV with low $j(O^1D)$, the over-prediction of modeled $P(O_3)$ and the elevated monoterpenes implies that the reactions of monoterpenes with O_3 may over-predict the formation of peroxy radicals. Budget analysis shows that $P(O_3)$ is dominated by the HO_2+NO reaction and followed by the MO_2+NO reaction in all regimes. Meanwhile, the ratio of the percent contribution of the HO_2+NO reaction to the sum of RO_2+NO reactions decreases as Φ increases, implying a decrease efficiency of the RO_2 to HO_2 conversion via the reaction of RO_2 with NO. Further analysis ascertain a declining sensitivity of $P(O_3)$ to HC

ACPD
10, 10551–10587, 2010

but ascending one to NO with Φ shifting from Regime II to Regime IV, according with the results from the indicator. Sensitivity studies for $P(O_3)$ are performed to discover the impaction of NO_x and monoterpenes on ozone production in different regions and to compare with the indicator representation. Expected results are obtained and are in good agreement with those given by the indicator. Therefore, the indicator can be applicable to illuminate the features of $P(O_3)$ sensitivity at the site.

1 Introduction

Tropospheric ozone is a major constituent of air pollution which is detrimental to human and vegetation (WMO, 1999). Ozone is also a green house gas in the upper troposphere and has an important impact on the radiative balance of the atmosphere (Brasseur et al., 1998). The concentration of surface ozone in the Northern Hemisphere has increased by a factor of 2 and more in average since the preindustrial era (Bojkov et al., 1988). Previously, it was assumed that tropospheric ozone comes from the stratosphere; however recent works have showed that a large fraction of the tropospheric ozone is due to in-situ photochemical production in rural and remote environment (Monks et al., 2000). High tropospheric ozone has been a great problem in many parts of the world (Frank et al., 2001). To develop effective abatement strategic, it is necessary to investigate whether the ozone production is controlled by HC, NO_x or both.

Kleinman et al. (1997) gave an analytic expression of the relative sensitivity of ozone production to changes in NO and HC (hydrocarbons, which include CH_4, CO, anthropogenic and biogenic hydrocarbons), which can be used to reveal the limiting factor for ozone formation. The relative sensitivity of $P(O_3)$ to [NO] and [HC], $d\ln P(O_3)/d\ln[NO]$ and $d\ln P(O_3)/d\ln[HC]$, which are defined as:

$$d\ln P(O_3)/d\ln[NO] = (1 - 3/2L_N/Q)/(1 - 1/2L_N/Q) \quad (1)$$

$$d\ln P(O_3)/d\ln[HC] = (1/2L_N/Q)/(1 - 1/2L_N/Q) \quad (2)$$

ACPD
10, 10551–10587, 2010

$$Q = 2k_1[HO_2]^2 + 2k_2[HO_2][RO_2] + L_R + L_N \quad (3)$$

where k_1 and k_2 are rate constant for the reactions of HO_2+HO_2 and HO_2+RO_2, L_R represents all radical-other radical reactions including HO+HO_2 and RO_2+$R'O_2$, L_N includes all radical loss reactions between free radicals and NO or NO_2 including HO+NO_2→HNO_3 and RO_2+NO → organic nitrate(Kleinman et al., 1997). Four distinctive regimes for $P(O_3)$ sensitivity can be obtained basing on the values of $d\ln P(O_3)/d\ln[NO]$ and $d\ln P(O_3)/d\ln[HC]$ (as shown in Fig. 4). Before analyzing the characteristics of $P(O_3)$ sensitivity these regions, it is worth summarizing the relevant chemistry of ozone formation.

Essential for the ozone formation is the cycle of odd hydrogen (odd H) which can be defined as the sum of OH, HO_2, and RO_2 (Kleinman et al., 1986, 1991). During daytime, sources of hydroxyl radicals are the photolysis of ozone, of nitrous, of aldehydes and of alkenes which can be an important OH source in rural areas (Platt et al., 1986; Alicke et al., 2003; Paulson et al., 1996; Ariya et al., 2000):

$$O_3 + h\nu \rightarrow O(^1D) + O_2 \quad (R1)$$

$$O(^1D) + H_2O \rightarrow 2OH \quad (R2)$$

These formation paths lead to daytime OH levels in the rang of several 10^6 cm^{-3} (Hein et al., 1997; Holland et al., 1998, 2003; Andreas et al., 2003). OH radical reacts with inorganic and organic species to oxidize them, leading to HO_2 and a variety of organic peroxy radicals which either react with NO to convert it to NO_2:

$$OH + CO \rightarrow HO_2 + CO_2 \quad (R3)$$

$$OH + VOC \rightarrow RO_2 + H_2O \quad (R4)$$

$$RO_2 + NO \rightarrow HO_2 + R'O_2 + NO_2 + \text{oxygenate VOC} \quad (R5)$$

$$HO_2 + NO \rightarrow NO_2 + OH \quad (R6)$$

ACPD
10, 10551–10587, 2010

The conversion of NO to NO_2 and the subsequent photolysis of NO_2 drive the ozone production:

$$NO_2 + h\nu \rightarrow O(^3P) + NO \quad \text{(R7)}$$

$$O(^3P) + O_2 \rightarrow O_3 \quad \text{(R8)}$$

Other reactions of OH with NO_x provide stable products and remove OH from the system:

$$OH + NO_2 \rightarrow HNO_3 \quad \text{(R9)}$$

$$OH + NO \rightarrow HONO \quad \text{(R10)}$$

The reactions of peroxy radicals with peroxy radicals also remove peroxy radicals from the system:

$$HO_2 + RO_2 \rightarrow ROOH + O_2 \quad \text{(R11)}$$

$$HO_2 + HO_2 \rightarrow H_2O_2 + O_2 \quad \text{(R12)}$$

In the cycle of odd hydrogen, NO_x compete with hydrocarbons (HC) for OH via Reactions (R9) and (R10), which can remove OH and retard peroxy radicals, and O_3 formation furtherly. NO also compete with peroxy radicals for peroxy radicals via Reactions (R5) and (R6), which can accelerate the conversion of NO to NO_2 and favor O_3 formation. Therefore, the production of ozone and its sensitivity to HC and NO_x changes greatly depend on those competitive reactions.

In Regime I, $d\ln P(O_3)/d\ln[NO]$ and $d\ln P(O_3)/d\ln[HC]$ are nearly constant and close to −1 and 1, separately. It indicates that $P(O_3)$ is greatly sensitive to both NO and HC, and $P(O_3)$ is negatively correlate with NO but positively with HC. Under high NO_x condition, OH radical dominantly reacts with NO_x which provides stable products due to high NO_x, leading to a very limited amount of peroxy radicals produced in the system. In such case, peroxy radicals react nearly completely with NO, and $P(O_3)$ is limited

ACPD
10, 10551–10587, 2010

by the peroxy radical concentrations. Then, an increase of the NO_x concentrations can decrease peroxy radicals concentrations clearly but cannot increase the NO to NO_2 conversion speed obviously, leading to a decrease of ozone production. However, an increase of HC concentrations can increase the loss of OH via HC, improve peroxy radicals concentrations and increase the production rate of ozone. Thus $P(O_3)$ is greatly sensitive to HC but negative sensitive to NO_x in this region. In Regime II, $d\ln P(O_3)/d\ln[NO]$ and $d\ln P(O_3)/d\ln[HC]$ vary from −1 to 0 and 1 to 0.5, separately, implying a declining sensitivity of $P(O_3)$ to HC and NO_x. In this regime, more OH radical is loss by the OH+HC reactions than the OH+NO_x reactions. Then a decrease of NO_x and an increase of HC both can not improve peroxy radicals effectively like them in Regime I, leading a less sensitivity of $P(O_3)$ to both HC and NO_x than Regime I. In Regime III, both $d\ln P(O_3)/d\ln[NO]$ and $d\ln P(O_3)/d\ln[HC]$ are greater than zero which means that $P(O_3)$ is positive sensitive to HC and NO. HC+OH reactions are the dominantly OH loss reactions due to a low NO_x concentration. The reaction of OH with HC produces sufficient peroxy radicals, which leads to the self- and cross-reactions become the important peroxy radicals loss reactions. For this situation the NO to NO_2 conversion are controlled by both NO and peroxy radicals concentrations and the effect of NO is more important, which is completely different with Regime I and Regime II. Therefore, the increase of the concentration of NO_x and HC cause an acceleration of the NO to NO_2 conversion speed and increase the production of ozone. Correspondingly, $P(O_3)$ is positive sensitive to both NO_x and HC in this regime. For the situation of high HC and low NO_x in Regime IV, the value of $d\ln P(O_3)/d\ln[NO]$ and $d\ln P(O_3)/d\ln[HC]$ is close to 1 and zero. HC+OH reactions are the dominantly OH loss reactions and peroxy radicals are almost removed via their self- and cross-reactions. The NO to NO_2 conversion speed is limited by the amount of available NO, so an increase of NO_x concentration can enhance O_3 formation effectively. Contrastively, an increase of HC concentration cannot increase O_3 production obviously, limited by the amount of available NO. Thus the ozone production rate is greatly sensitive to NO_x but insensitive to HC.

ACPD
10, 10551–10587, 2010

From the above analysis, the sensitivity of $P(O_3)$ is determined by the proportions of OH radical reacting with HC and peroxy radicals reacting with NO, relating to the parameter Φ which describes the competition between NO_x and HC for OH:

$$\Phi = k_{HC+OH}[HC]/k_{NO_x+OH}[NO_x] \quad (4)$$

where k_{HC+OH} and k_{NO_x+OH} are the combined rate coefficient for the reactions of OH radical with HC and NO_x separately. [HC], [NO] and [NO_2] are the concentration of HC, NO and NO_2, separately. The ozone production rate, $P(O_3)$, depends on the concentrations of peroxy radicals (HO_2+RO_2) and NO. The production of peroxy radical is linked to the value of $k_{HC+OH}[HC]$, while NO concentration is linked to the NO_x concentration and therefore the value of $k_{NO_x+OH}[NO_x]$. Thus Φ can be used for identifying the sensitivity of $P(O_3)$ to NO_x and HC. Φ is compatible with the indicator Θ proposed by (Frank et al., 2001), which was defined as the ratio of the lifetimes of OH against the losses by reacting with VOCs and NO_x. If HC concentrations except CH_4 and CO were used in calculating the value of Φ, there exists a reciprocal relation between the values of Φ and the indicator Θ. The addition of CH_4 and CO in our work was based on three considerations. Firstly, both CH_4 and CO can react with OH radical to produce peroxy radicals (CH_3O_2 for CH_4, and HO_2 for CO) which are similar with VOCs. Secondly, they have been included in hydrocarbons for testing the relative sensitivity of $P(O_3)$ to HC and NO_x. The most important reason is to facilitate the analysis, for a value of Φ being one unit means an equal proportion of OH to react with HC to produce peroxy radicals and to react with NO_x to provide stable products.

In this paper, we will investigate the parameter Φ as an indicator to determine the sensitivity of ozone production to HC and NO_x and to analyze the behavior of $P(O_3)$ in different sensitive regions using the data from RISFEX 2003 (RIShiri Fall EXperiment 2003) campaign conducted in September 2003 at Rishiri Island (45.07° N, 141.12° E, and 35 m a.s.l.) in the sea of Japan. Furth more, a box model based on RACM was used to investigate the robustness of the indicator.

ACPD
10, 10551–10587, 2010

2 Experimental

The measurements were conducted at an observatory (Rishiri Island Observatory, RIO) (45.07° N, 141.12° E, 35 m a.s.l.) built on Rishiri island, which is a round dormant volcanic island with a diameter of ca. 15 km and ca. 20 km northwest of Hokkaido in the sea of Japan. In its center stands a 1721 m high mountain covered by a coniferous forest on its slope. RIO is situated on a foothill of the mountain ca. 800 m away from the shore (Fig. 1). The population on the island is ca. 7500 and local pollution can be negligible (Tanimoto et al., 2000). Previous study at Rishiri Island has shown that the site receives the air masses usually from the clean Arctic, West Siberia and Pacific region as well as from polluted Japan and continental Asia (Tanimoto et al., 2000).

In the observatory, there were two 2-m high containers used to house instruments and the inlets for trace gas and aerosol measurements. Peroxy radicals were measured by PERCA technique (Cantrell et al., 1982). The inlet of the PERCA instrument was mounted on the top of a container. NO and NO_2 were measured by a chemiluminescence instrument with a photolytic converter (CLD770AL and PLC760, Eco Physics). The detection limits for NO and NO_2 measurement were 22 and 45 pptv (S/N=2, 1-min measurement time), respectively. O_3 was measured by a commercial UV absorption analyzer (49C, Thermo). CO was measured with a non-dispersive infrared (NDIR) photometer instrument (48C, Thermo). Black carbon was measured with a commercial instrument based on absorption photometry (AE-21, Magee Scientific). Non-methane hydrocarbons (NMHCs) were measured by GC-FID and GC-MS followed by sampling the air into canisters. HCHO, CH_3CHO, acetone, toluene, and monoterpenes were measured by proton-transfer reaction-mass spectrometry (PTR-MS). Speciation and quantification of monoterpenes were made with two GC-based instruments. The solar actinic flux and photolysis frequency of O_3 to $O(^1D)$ ($j(O^1D)$) and NO_2 to NO ($j(NO_2)$) were measured by an actinic flux spectral radiometer(GmbH, Meteorologie Consult). The atmospheric aerosols were measured using a scanning mobility particle sizer (Model 3936, TSI) and an optical particle counter (KC18, Rion).

Temperature, relative humidity, pressure, and wind direction and speed were recorded with conventional meteorological instruments. Further detailed description of the measurements and instruments has been given elsewhere (Qi et al., 2007).

3 Model

A time-dependent box model based on Regional Atmospheric Chemistry Modeling (RACM) (Stockwell et al., 1997) was developed to describe the remote MBL chemistry and to calculate HO_2 and RO_2 concentrations. Kinetic rate constants were updated using the results in (Sander et al., 2003). The model was also updated by incorporating with more detailed monoterpenes chemistry (Qi et al., 2007). The running of the model was constrained with measured stable chemical species, photolysis frequencies and meteorological parameters with the integrations conducting each day for 24 h starting at 00:00 and ending 24:00 JST (Japan standard time) at 10-min intervals given the measurement data available. If time resolution of the measurements was greater or less than once every 10 min, averaging or linear interpolation was used to calculate the input data. In daytime, the 1σ uncertainty of the model, based on the combined uncertainties in the kinetic rate coefficients and in the measured concentrations of species, was estimated using a Monte Caro approach to be ca. ±30% (Carslaw et al., 1999).

4 Result and discussion

4.1 Ozone production rate ($P(O_3)$) during the campaign

The ozone production rate, $P(O_3)$, can be approximately determined by the rate at which NO is oxidized to NO_2 by the reaction with peroxy radicals (Kleinman et al., 1995):

$$P(O_3) = k[NO]([HO_2] + [RO_2]) \quad (5)$$

where k is a combined rate coefficient for the oxidation of NO to NO_2 by all peroxy radicals. In this approach, the minor pathway of the higher organic peroxy radicals that lead to formation of organic nitrates and the loss of NO_2 by reaction with OH are neglected, thus Eq. (5) represents an upper limit for $P(O_3)$ (Mihelcic et al., 2003). $P(O_3)$ is estimated by the observed HO_2 and RO_2 concentration (Fig. 2a).

During RISFEX2003, the data coverage allows for determination of the ozone production rate during 18–21 September. The daytime weather during the period was typically clear in the morning hours (06:00–11:00 JST), and scattered clouds frequently appeared overhead at noon and in the afternoon as shown in Fig. 2d. The daytime is defined as the interval of $j(O^1D)>1\times10^{-7}\,s^{-1}$, corresponding to time from 06:00 to 18:00 JST. The local wind direction at the site was dominated by the south in daytime and shifted to the north in the night, exhibiting typical land-sea breeze.

The time series of ozone production rate together with pertinent chemical species and physical parameters in 10-min averages is shown in Fig. 2. Figure 2b shows that RO_x (the sum of HO_2, RO_2 and OH radicals) signals increase quickly in the early morning on clear-sky days, and reach a peak at ~11:50 JST. In the afternoon, the radical signals decay consistently with the attenuation of UV radiation flux. In contrast, little variation is observed on the cloudy day (19 September). This suggests that the production of peroxy radicals is strongly driven by photochemistry same as the previous observations in MBL (Burkert et al., 2001; Carpenter et al., 1997).

We can see from Fig. 2a that ozone production rate varies greatly between days, with midday values (10-min average) varying from 0.1 to 8.7 ppbv h^{-1} (ppbv refers to part per billion by volume, same hereinafter). The scatter in $P(O_3)$ is primarily caused by NO since NO was more variable than RO_x. The high $P(O_3)$ occurring on 18 September is due to both high NO and peroxy radical levels. The daily mean $P(O_3)$ for all data determined in this work is 0.93, similar with reported values obtained in MBL (Salisbury et al., 2002; Monks et al., 1998; Fleming et al., 2006). The value of Φ, calculated using the observed data of HC species and NO_x concentrations, varies in the rang of 3.9–107.2, with no distinct diurnal variation (Fig. 2e).

ACPD
10, 10551–10587, 2010

4.2 Sensitivity of $P(O_3)$ to HC and NO_x

Figure 3 shows the dependence of $P(O_3)$ on Φ. A modeled trend of $P(O_3)$ with increasing Φ was also shown in Fig. 3, which is similar with the variation of observed $P(O_3)$ vs. Φ. The running of the model is under the condition that the concentrations of all chemical species except for NO and NO_2 and physical parameters are constrained to those measured at 11:50 JST on 18 September. With the ratio of NO to NO_2 invariable, we change the concentration of NO and NO_2 to obtain a series of different Φ in the range of 0.01–1000. Obviously, the variation of $P(O_3)$ could be divided into two different trends as Φ change. When Φ is very low (Regime II), $P(O_3)$ increases as Φ increases, indicating a positive correlation between $P(O_3)$ and Φ. When Φ reached to a critical value, known as Φ_{opt}, there exists a maximum amount of $P(O_3)$ in the process of the continual increase of Φ. At $\Phi>\Phi_{opt}$, $P(O_3)$ was found to be negatively correlated with Φ. We also calculated the relative sensitivity of $P(O_3)$ to [NO] and [HC] to indicate $P(O_3)$ sensitivity clearly. The results of $P(O_3)$, $d\ln P(O_3)/d\ln[NO]$ and $d\ln P(O_3)/d\ln[HC]$ are shown in Fig. 4. As shown by Fig. 4, it is clearly that the sensitivity of $P(O_3)$ to HC and NO_x changes can be divided into four regions discussed in the beginning of this article. The range of observed Φ is in Regime II, III and IV. In Regime II ($\Phi<\Phi_{opt}$), $P(O_3)$ is negative sensitive to NO and thus positively related with Φ. Oppositely, $P(O_3)$ is positive sensitive to NO and shows a negative correlation with Φ in Regime III and IV ($\Phi>\Phi_{opt}$).

By comparing the results from this study to those from other studies (Milford et al., 1994; Frank et al., 2001), the definitions of the regimes were greatly different. Milford (1994) distinguished only between two regimes. Ozone production is considered to be NO_x limited when $d\ln P(O_3)/d\ln[NO]>d\ln P(O_3)/d\ln[HC]$, otherwise it is HC limited. They classified Regime I, II and parts of Regime III to the HC-limited regime and other parts of Regime III and whole Regime IV to the HC regime. From this classification $P(O_3)$ in Regime I is HC limited, therefore, ozone abatement must rely on the reduction of HC concentration. However, basing on the former analysis, a rise of NO_x

also can reduce the production of ozone in this region. In the work (Frank et al., 2001), $P(O_3)$ was distinguished between three regimes, and the definition of Regime II and Regime III were same as Regime III and Regime IV in our study, separately. The difference is that they classified Regime I and Regime II into one region. However, it is clear that the competition for OH between HC and NO_x, and the $P(O_3)$ sensitivity for HC and NO_x, are completely different in Regime I and Regime II.

Although the relative sensitivity of $P(O_3)$ can identify ozone production sensitive regions exactly, the calculation of the values using Eqs. (1) and (2) was more complex. In Fig. 5, the calculated values of $d\ln P(O_3)/d\ln[NO]$ and $d\ln P(O_3)/d\ln[HC]$ from the model are plotted against 10-min averaged Φ calculated by the observed concentrations of HC and NO_x. From Fig. 4 and Fig. 5, it is undoubtedly that there is a good correlation between Φ and $d\ln P(O_3)/d\ln[NO]$ (or $d\ln P(O_3)/d\ln[HC]$), and the value of Φ is easy obtained than the other two. Thus Φ is an more convenient parameter to indicating the sensitivity of $P(O_3)$ to HC and NO_x. However, the relationship between the relative sensitivity and Φ is not directly affected by NO and L(HC) (Fig. 5a and b), which further proved that the sensitivity of ozone production is determined by the ratio rather than the concentrations of NO_x or HC.

In this work, the border between Regime I and Regime II is defined as Φ=1, which indicates a comparable competition for OH between HC and NO_x. The border between Regime II and Regime III, known as Φ_{opt}, is defined as the value of Φ at which $d\ln P(O_3)/d\ln[NO]$ equal to zero. The border between Regime III and Regime IV is defined as the value of Φ at which the ratio of $d\ln P(O_3)/d\ln[HC]$ to $d\ln P(O_3)/d\ln[NO]$ is lower than 0.05. During our observation, Φ_{opt} is ca. 7±3, which agrees with the conclusion in (Tonnesen et al., 2000; Frank et al., 2001). The value of Φ at the third border is ca. 23±7, which is comparable to the result in (Frank et al., 2001). During the campaign, there are 24, 127 and 120 data points located in Regime II, III and IV, respectively. Regime I was not observed. In estimation, Regime I could appear at a high NO_x level, especially high NO_2 level.

ACPD
10, 10551–10587, 2010

4.3 Robustness study of Φ

As discussed in Frank et al. (2001), the indicator Θ can be used to find instantaneous sensitivity regime of an air parcel, in contradistinction to other earlier proposed indicator based on long-lived species. More importantly, it is more robust than the indicators NO_y and O_3/NO_z and of comparable robustness as the indicator H_2O_2/HNO_3. As an improved parameter based on the indicator Θ, Φ inherits the advantages of the original indicator, but it also has the largest problem from very high percentages of large alkenes. Fortunately, the studied site is far free from impact of human activities, thus the emission of alkenes which are mainly emitted from diesel motors is greatly limited. Therefore, the improved indicator Φ is suitable for ascertaining the sensitivity region of $P(O_3)$ in this island. However, due to the addition of CH_4 and CO concentrations in determining the value of Φ, it is necessary to test the robustness of the indicator.

Firstly, model calculations were used to study the effect of the atmospheric compositions of VOCs on the value of Φ_{opt}. We separately increase the observed concentration of the selected VOC species by a factor of 1.5 and holding other VOCs constant, to calculate $P(O_3)$ at different binned Φ and determine the value of Φ_{opt}. The performing of the calculations is similar with the former. By comparing those Φ_{opt} values with the initial Φ_{opt} calculated by the observed data, we obtain the Φ_{opt} change ($\Delta\Phi_{opt}$) due to the increase of VOCs concentration. The results are shown in Fig. 6. As Fig. 6a shows, the increase of ISO concentration for 50% lead to a 2.2% increase of Φ_{opt}, which is greater than other VOCs. The following VOCs are MACR, TOL and ALD. Others such as HCHO, monoterpenes, and KET lead very little change of Φ_{opt}. Moreover, the increase of ISO, ALD, HCHO and monoterpenes lead to Φ_{opt} increase but the increase of KET, TOL and MACR reduce Φ_{opt}. We also calculated the change of Φ_{opt} with one unit (ppbv) of VOCs increase (Fig. 6b). From Fig. 6b, it is clear that the increase of ISO, ALD, monoterpenes, TOL, and MACR lead to a great change of Φ_{opt}. Thus, BVOCs (ISO and monoterpenes) emitted from local plants will increase the value of Φ_{opt}, but TOL from anthropogenic and MACR from the sea will reduce Φ_{opt}, implying that the

ACPD
10, 10551–10587, 2010

local Φ_{opt} is higher than those in low BVOCs and more polluted environments.

The values of Φ_{opt} are found to be correlated with OH concentration and the NO/NO_2 ratio (Fig. 5c and d). Model results show that the factors which can improve the OH production rate, such as O_3 concentration, humidity, $j(O^1D)$ etc., will lead to a decrease of Φ_{opt} (Figs. 7 and 8). As Fig. 7a shows, the variations of $P(O_3)$ with increasing Φ show same tendency at each fixed concentration of O_3. In all cases, $P(O_3)$ increase with the increase of Φ at $\Phi < \Phi_{opt}$ and reach the maximum value at Φ_{opt}. At $\Phi > \Phi_{opt}$, the farther increase of Φ lead to $P(O_3)$ decrease. When the concentration of O_3 is constrained to 1 ppbv, the value of Φ_{opt} is about 5. Φ_{opt} decrease to a value of 2.5 when the O_3 concentration increase to 100 ppbv. It implies a negative correlation between ozone concentrations and Φ_{opt}. In Fig. 7, we also use different color to show the level of OH radical. It is clear that a high O_3 concentration leads to a high OH level. And there shows a negative correlation between the concentration of OH and Φ_{opt}. The results shown by Fig. 7b are similar as the former. Form Fig. 7, it is observed that the concentration of OH at the point of Φ_{opt} is about 0.1 pptv in the condition of high photolysis rate and 1 ppbv O_3, which is close to that in the condition of low photolysis rate and 100 ppbv O_3. The corresponding Φ_{opt} in the two conditions are comparable and equal to 5. The phenomena imply a fact that the value of Φ_{opt} is related to the concentration of OH, and the increase of OH concentration will reduce Φ_{opt}. Figure 8 shows the dependence of $P(O_3)$ on Φ when the relative humidity is constrained to 10% (shown by point), 20% (shown by plus sign), 50% (shown by asterisk) and 90% (shown by cross), respectively. As shown by Fig. 8a, there exit same tendency of $P(O_3)$ with Φ at four different value of relative humidity. When the relative humidity is constrained to 10%, the value of Φ_{opt} is about 4.5. Φ_{opt} decrease to a value of 4 when the relative humidity increase to 90%. From Fig. 8a, it is indicated that the increase of the relative humidity leads to the increase of OH concentration and the decrease of Φ_{opt}. Figure 8b shows the results in low photolysis rate. It is observed that there is not clear difference in the vary of $P(O_3)$ when the relative humidity is constrained to different values. Due to the low photolysis rate, the increase of relative humidity cannot

ACPD
10, 10551–10587, 2010

effectively improve the concentration of OH radical (Fig. 8b), thus the value of Φ_{opt} is invariable with the increase of relative humidity. By above analysis, the inherent factor influencing the value of Φ_{opt} is OH radical rather than the initial concentration of ozone, relative humidity and $j(O^1D)$.

We also calculated Φ_{opt} in different NO/NO_2 ratio conditions. The results are shown in Fig. 9. The value of Φ_{opt} is about 4 at a greatly low NO/NO_2 ratio (NO/NO_2=0.01), and the corresponding maximum $P(O_3)$ is very low due to the high NO_2. At a greatly high NO/NO_2 ratio (NO/NO_2=100), Φ_{opt} is close to 10 and the corresponding maximum $P(O_3)$ is about 7.5 ppbv/h. Form Fig. 9, it is clearly that the decrease of the NO/NO_2 ratio lead to Φ_{opt} decrease. Moreover, the maximum $P(O_3)$ is also decrease with the decreasing of NO/NO_2. In the fast photochemical cycling of NO_x in daytime, the NO/NO_2 ratio is determined by the concentration of O_3 and peroxy radicals as well as $j(NO_2)$ (Cadle et al., 1952; Leighton et al., 1961; Crawford et al., 1996):

$$\frac{[NO_2]}{[NO]} = \frac{(k_1[O_3] + k_2[HO_2] + k_3[RO_2])}{j(NO_2)} \quad (6)$$

where k_1, k_2 and k_3 c with O_3, HO_2 and RO_2, separately. $j(NO_2)$ is the photolysis rate of NO_2. Equation (6) is proved to be suitable for remote locations (McFarland et al., 1978; Ritter et al., 1979; Fehsenfeld et al., 1983; Parrish et al., 1986; Trainer et al., 1987). From Eq. (6), it is obviously that high O_3 and peroxy radicals concentrations will lead to low NO/NO_2 ratio. Therefore, O_3 can impact Φ_{opt} by two processes: one is that the increase of O_3 will improve the OH level and reduce Φ_{opt}, another is that the increase of O_3 will reduce the NO/NO_2 ratio and reduce Φ_{opt} value furtherly.

As mentioned above, the value of Φ_{opt} is impacted by the local atmospheric composition of VOCs, ozone concentration, humidity, photolysis rate and the NO/NO_2 ratio. However, Φ_{opt} has been fluctuating within a small range from 4 to 10 in all case studies, indicating that Φ is robust against those parameters.

ACPD
10, 10551–10587, 2010

4.4 Behavior of $P(O_3)$ in different regimes

The ozone production rate was estimated additionally using the peroxy radicals derived from the model using Eq. (5). The results are shown in Fig. 10. Basically, the modeled $P(O_3)$ track the diurnal and day to day variation of experimental $P(O_3)$ well. The $P(O_3)_{exp}/P(O_3)_{mod}$ rate is obviously higher than one unit when Φ is lower than 10 (Regime II), especially at high $j(O^1D)$ ($j(O^1D)>10^{-6}$). Moreover, the values of $d\ln P(O_3)/d\ln[HC]$ are commonly higher than 0.8, implying that the model tends to underestimate $P(O_3)$ when $P(O_3)$ is greatly sensitive to HC. It indicates an important source of RO_2 of unknown reactive BVOCs is missed, as mentioned by (Qi et al., 2007). The underestimate trend became weaker at $\Phi>30$ (Regime IV) for $P(O_3)$ is less sensitive to HC. In this region, however, the $P(O_3)_{exp}/P(O_3)_{mod}$ rate is commonly lower than one unit at low $j(O^1D)$ ($j(O^1D)<10^{-6}$), implying that our model maybe overestimate the production of peroxy radicals which is not formed by photochemistry. Due to the high concentrations of BVOCs in the early morning and late afternoon (low $j(O^1D)$) (Qi et al., 2007), it indicates that the reactions of BVOCs (especially monoterpenes) with O_3 maybe over-predict the formation of peroxy radicals from the reactions.

Figure 12 shows the itemization of $P(O_3)$ calculated for different Regimes. As Fig. 12 shows, the average $P(O_3)$ is 3.22 ppbv/h in Regime II, 2.07 ppbv/h in Regime III and 0.78 ppbv/h in Regime IV, separately, which illuminates a decreasing trend of $P(O_3)$ with increasing Φ. In all Regimes, $P(O_3)$ is dominated by the HO_2+NO reaction and followed by the MO_2+NO reaction. The two reactions contribute ca. 69% and 16% in Regime II, 67% and 17% in Regime III, 66% and 19% in Regime IV, separately. Reactions of other peroxy radicals with NO contribute very little. As Φ increases, the ratio of the percent contribution of the HO_2+NO reaction to the sum of RO_2+NO reactions decrease, indicating a decrease of the efficiency of the RO_2 to HO_2 conversion via the reaction of RO_2 with NO. All RO_2+NO reactions shows an increasing trend when Φ vary from Regime II to IV, except for an abnormally high contribution of TERP+NO in Regime II and ISOP+NO in Regime III, leading by the high OH reactivity due to

monoterpenes (L(TER)) and Isoprene (L(ISO)) in corresponding regimes. The values of L(TER), NO concentration and the averaged $P(O_3)$ formed by monoterpenes+NO reactions in Regime II are higher than them in Regime IV by a factor of 1.16, 14.25 and 5.76, implying the effect of NO on $P(O_3)$ is weaker in Regime II than it in Regime IV. For Isoprene, the corresponding values in Regime III are higher than them in Regime IV by a factor of 1.36, 3.45 and 2.93, revealing the effect of NO on $P(O_3)$ in Regime III is weaker than it in Regime IV. The above data provide confidence that the ozone production rate is more sensitive to NO in Regime IV than it in Regime II and III.

As Fig. 12 shows, the 10-min average $P(O_3)$ data are categorized into 3 classes by $j(O^1D)$ (s^{-1}) value: (1) $j(O^1D)<10^{-6}\,s^{-1}$ (signaled as J1), (2) $10^{-5}\,s^{-1} > j(O^1D)>10^{-6}\,s^{-1}$ (signaled as J2), and (3) $j(O^1D)>10^{-5}\,s^{-1}$ (signaled as J3) in each regimes. In Regime II, the average value of $P(O_3)$ is 0.28 ppbv/h at J1, 0.74 ppbv/h at J2 and 2.20 ppbv/h at J3, separately. As $j(O^1D)$ increase, $P(O_3)$ in Regime II increases greatly, which is caused by the increasing peroxy radicals concentrations, indicating that the concentrations of peroxy radicals are important factor to control the O_3 production in Regime II, thus $P(O_3)$ is sensitive to L(HC) as well as HC. In Regime III and Regime IV, the average value of $P(O_3)$ is 0.21 and 0.06 ppbv/h at J1 level, 0.53 and 0.20 ppbv/h at J2 level and 1.33 and 0.51 ppbv/h at J3 level, separately. In those two regimes, the increase of $P(O_3)$ (especially in Regime IV) caused by increasing $j(O^1D)$ is clearly less than that in Regime II. The above data indicate that the effect of peroxy radicals to control O_3 production becomes weaker with increasing Φ, implying a declining sensitivity of $P(O_3)$ to HC. In the condition of J1 in Regime IV, the percent contribution of monoterpenes+NO reactions for $P(O_3)$ is clearly higher than it in other conditions, for a completely high concentrations of monoterpenes in this region. In such case, the monoterpenes+O_3 reactions may be significant for peroxy radicals production. The formed peroxy radicals can not conversion to HO_2 radical efficiently in low NO condition, which can explain the low percent contribution of HO_2+NO reaction. Moreover, a low $P(O_3)_{exp}/P(O_3)_{mod}$ rate found in this region imply that the reactions of BVOCs (especially monoterpenes) with O_3 maybe over-predict the formation of peroxy

radicals from the reactions (Fig. 11).

The island is located in the sea of Japan and is far free from impact of human activities. However, the plants are abundant over the island, thus the emission of BVOCs such as isoprene and monoterpenes can be significant (Tanimoto et al., 2000; Kanaya et al., 2002a, b). To find the controlling factor for ozone production, it is necessary to analyze the $P(O_3)$ sensitivity to BVOCs and NO_x. Firstly, sensitivity runs for $P(O_3)$ are performed by changing NO_x and monoterpenes concentrations. In the calculations, ozone and its precursors except for NO_x and monoterpenes are basically constrained to those observed at for selected times in our observation. Each run is performed with the sum mixing ratio of NO_x fixed at a value between 1 pptv to 100 ppbv, and the NO/NO_2 ratio is constrained to it observed at the selected time. Monoterpenes concentration is fixed at a value between 1 pptv to 1 ppbv, covering the concentration range observed during our campaign. The model results are shown in Fig. 13.

At 08:40 JST on 18 Septermber, the mixing ratio of NO_x and monoterpenes is 909 pptv and 48 pptv, separately. The value of the indicator is 9.54 ($d\ln P(O_3)/d\ln[NO]$ is close to zero and $d\ln P(O_3)/d\ln[HC]$ is about 0.5), which indicate that the system is situated on the border between Regime II and Regime III, and $P(O_3)$ in the selected area is sensitive to monoterpenes change but not sensitive to NO_x (Fig. 13a). At 13:10 JST on 21 September, the mixing ratio of NO_x and monoterpenes are 93 pptv and 3 pptv, separately. With Φ value of 77.39, it indicate that the system is in Regime IV, and $P(O_3)$ in the selected area is sensitive to NO_x change but not sensitive to monoterpenes (Fig. 13b). At 13:00 JST on 20 September, the mixing ratio of NO_x and monoterpenes are 1280 pptv and 39 pptv, separately. $P(O_3)$ is in Regime II (Φ=5.57) and is sensitive to monoterpenes and NO_x change (Fig. 13c). At 06:40 JST on 21 September, the mixing ratio of NO_x and monoterpenes are 482 pptv and 172 pptv, separately. The value of Φ is equal to 14.18 with a comparable values of $d\ln P(O_3)/d\ln[NO]$ and $d\ln P(O_3)/d\ln[HC]$, indicating that the system is in Regime III and $P(O_3)$ in the selected area is sensitive to monoterpenes change and NO_x change (Fig. 13d). We also test the $P(O_3)$ sensitivity to NO_x and Isoprene change, the result is similar. Results form

ACPD
10, 10551–10587, 2010

sensitivity studies indicate the $P(O_3)$ sensitivity to NO_x and HC in four regimes clearly, which is greatly agree with the results from the indicator.

5 Conclusions

In this work, we developed an improved indicator $\Phi=k_{HC+OH}[HC]/k_{NO_x+OH}[NO_x]$ to study the $P(O_3)$ sensitivity to HC and NO_x in the field campaign RISFEX 2003 made in September 2003 at Rishiri island in the sea of Japan. Four different sensitivity regimes were given based on the indicator. $P(O_3)$ is located in Regime I at $\Phi<1$ while in Regime IV when Φ is larger than 23±7. The border between Regime II and Regime III, known as Φ_{opt}, is ca. 7±3. $P(O_3)$ was greatly sensitive to NO_x in Regime I and IV and to HC in Regime I but nearly insensitive to HC in Regime IV, while less sensitive to both HC and NO_x in other two regimes. Furthermore, there has a negative correlation between $P(O_3)$ and NO_x in Regime I and II but a positive one in the two later regimes, in contrast to a positive relationship between $P(O_3)$ and HC in all regimes. During the studied daytimes, there are 24, 127 and 120 data points located in Regime II, III and IV, respectively. It implies that approximately 91% of $P(O_3)$ data are located in NO_x positive sensitive region, illuminating that NO_x is a limiting factor for ozone production, thus a controlling of NO_x emission can be a more efficient strategy for ozone abatement at the site.

The experimental $P(O_3)$ are compared with those derived from model and give the result generally in an agreement. However, the model tends to underestimate $P(O_3)$ when $P(O_3)$ is greatly sensitive to HC in Regime II, but this underestimate trend became weaker at $\Phi>30$ for $P(O_3)$ is less sensitive to HC in Regime IV. The results indicate an important source of RO_2 of unknown reactive BVOCs is missed. In Regime IV, the $P(O_3)_{exp}/P(O_3)_{mod}$ rate is commonly lower than one unit at low $j(O^1D)$ ($j(O^1D)<10^{-6}$), implying that our model maybe overestimate the production of peroxy radicals which is not formed by photochemistry. Moreover, the greatly high monoterpenes in this region indicate that our current model maybe over-predict the formation

ACPD
10, 10551–10587, 2010

of peroxy radicals from the reactions of monoterpenes with ozone. Budget analysis shows that $P(O_3)$ is dominated by the HO_2+NO reaction and followed by the MO_2+NO reaction in all regimes. The two reactions contribute ca. 69% and 16% in Regime II, 67% and 17% in Regime III, 66% and 19% in Regime IV, separately. Reactions of other peroxy radicals with NO contribute very little. Meanwhile, the ratio of the percent contribution of the HO_2+NO reaction to the sum of RO_2+NO reactions decreases as Φ increases, implying a decrease efficiency of the RO_2 to HO_2 conversion via the reaction of RO_2 with NO. Moreover, it shows a declining sensitivity of $P(O_3)$ to HC but a ascending sensitivity of $P(O_3)$ to NO_x, when the situation shifted from Regime II to Regime IV. Sensitivity analysis indicated the sensitivity of $P(O_3)$ to NO_x/monoterpenes changes in different regimes, which show a completely agreement with the results from the new indicator. Those studies approve that the indictor is succeed to distinguish character of $P(O_3)$ sensitivity at the site.

References

Alicke, B., Geyer, A., Hofzumahaus, A., Holland, F., Konard, S., Pätz, H. W., Schäfer, J., Stutz, J., Andreas, V. T., and Platt, U.: OH formation by HONO photolysis during the BERLIOZ experiment, J. Geophy. Res., 108(D4), 8247, doi:10.1029/2001JD000579, 2003.

Ariya, P. A., Sander, R., and Crutzen, P. J.: Significance of HO_x and peroxides production due to alkene ozonolysis during fall and winter: A modeling study, J. Geophy. Res., 105, 17721–17739, 2000.

Bojkov, R. D.: Ozone changes at the surface and in the free troposphere, in: Tropospheric Ozone, edited by: Isaksen, I. S. A., Reidel, Dordrecht, 83–96, 1988.

Brasseur, G. J., Kiehl, T., Muller, J. F., Schneider, T., Granier, C., Tie, X. X., and Hauglustaine, D.: Past and future changes in global tropospheric ozone: Impact on radiative forcing, Geophys. Res. Lett., 25, 3807–3810, 1998.

Burkert, J., Andres, M. D., Stobener, D., Burrows, J. P., Weissenmayer, M., and Kraus, A.: Peroxy radical and related trace gas measurements in the boundary layer above the Atlantic Ocean, J. Geophys. Res., 106, 5457–5477, 2001.

Cadle, R. D. and Johnston, H. S.: Chemical reaction in Los Angeles smog, Proc. Natl, Air Pollution Symp., 2nd, 1952.

Calvert, J. G. and Stockwell, W. R.: Deviations from the O_3-NO-NO_2 photostationary state in tropospheric chemistry, Can. J. Chem., 61, 983–992, 1983.

Cantrell, C. A. and Stedman, D. H.: A possible technique for the measurement of atmospheric peroxy radicals, Geophys. Res. Lett., 9, 846–849, 1982.

Carpenter, L. J., Monks, P. S., Galbally, I. E., Meyer, C. P., Bandy, B. J., and Penkett, S. A.: A study of peroxy radicals and ozone photochemistry at coastal sites in the Northern and Southern Hemisphere, J. Geophys. Res., 102, 25417–25427, 1997.

Carlslaw, N., Jacoba, P. J., and Pilling, M. J.: Modeling OH, HO_2, and RO_2 radicals in the maring boundary layer 2. Mechanism reduction and uncertainty analysis, J. Geophys. Res., 104, 30257–30273, 1999.

Crawford, J. and Davis, D.: Photostationary state analysis of the NO-NO_2 system based on airborne observations from the western and central North Pacific, J. Geophy. Res., 101, 2053–2072, 1996.

Fehsenfeld, F. C., Bollinger, M. J., Liu, S. C., Parrish, D. D., McFarland, M., Trainer, M., Kley, D., Murphy, P. C., Albritton, D. L., and Lenschow, D. H.: A study of ozone in the Colorado mountains, J. Atmos. Chem., 1, 87–105, 1983.

Fleming, Z. L., Monks, P. S., Rickard, A. R., Heard, D. E., Bloss, W. J., Seakins, P. W., Still, T. J., Sommariva, R., Pilling, M. J., Morgan, R., Green, T. J., Brough, N., Mills, G. P., Penkett, S. A., Lewis, A. C., Lee, J. D., Saiz-Lopez, A., and Plane, J. M. C.: Peroxy radical chemistry and the control of ozone photochemistry at Mace Head, Ireland during the summer of 2002, Atmos. Chem. Phys., 6, 2193–2214, 2006, http://www.atmos-chem-phys.net/6/2193/2006/.

Frank, K., Francois, J., Alain, C., Bernd, K., Hubert, B., and Bertrand C.: Total VOC reactivity in the planetary boundary layer: 2. A new indicator for determining the sensitivity of the ozone production to VOC and NO_x, J. Geophy. Res., 106, 3095–3110, 2001.

Geyer, A., Bächmann, K., Hofzumahaus, A., Holland, F., Konrad S., Klüpfel, T., Pätz, H. W., Perner, D., Mihelcic, D., Schäfer, H. J., Andreas, V. T., and Platt, U.: Nighttime formation of peroxy and hydroxyl radicals during the BERLIOZ campaign: Observations and modeling studies, J. Geophy. Res., 108(D4), 8249, doi:10.1029/2001JD000656, 2003.

Hein, R., Crutzen, P. J., and Heimann, M.: An inverse modeling approach to investigate the global atmospheric methane cycle, Global Biogeochem. Cy., 11, 43–76, 1997.

Holland, F., Aschumutat, U., Hebling, M., Hofzumahaus, A., and Ehhalt, D. H.: Highly time resolved measurements of OH during POPCORN using laser-induced fluorescence spectroscopy, J. Atmos. Chem., 31, 205–225, 1998.

Holland, F., Hofzumahaus, A., Schäfer, J., Kraus, A., and Pätz, H. W.: Measurements of OH and HO_2 radical concentrations and photolysis frequencies during BERLIOZ, J. Geophy. Res., 108(D4), 8246, doi:10.1029/2001JD001393, 2003.

Kanaya, Y., Nakamura, K., Kato, S., Matsumoto, J., Tanimoto, H., and Akimoto, H.: Nighttime variations in HO_2 radical mixing ratios at Rishiri Island observed with elevated monoterpene mixing ratios, Atmos. Environ., 36, 4929–4940, 2002a,

Kanaya, Y., Yokouchi, Y., Matsumoto, J., Nakamura, K., Kato, S., Tanimoto, H., Furutani, H., Toyota, K., and Akimoto, H.: Implications of iodine chemistry for daytime HO2 levels at Rishiri Island, Geophys. Res. Lett., 29(8), 1212, doi:10.1029/2001GL014061, 2002b.

Kleinman, L. I.: Photochemical formation of peroxides in the boundary layer, J. Geophys. Res., 91, 10889–10904, 1986.

Kleinman, L. I.: Seasonal dependence of boundary layer peroxide concentration: The low- and high-NO_x regimes, J. Geophys. Res., 96, 20721–20734, 1991.

Kleinman, L. I., Lee, Y. N., Springston, S. R., Lee, J. H., Nunnermacker, L. J., Weinstein, J. L., Zhou, X., and Newman, L.: Peroxy radical concentration and ozone formation rate at a rural site in southeastern United States, J. Geophys. Res., 100, 7263–7273, 1995.

Kleinman, L. I., Daum, P. H., Lee, J. H., Lee, Y. N., Nunnermacker, L. J., Springston, S. R., Newman, L., Judith, W. L., and Sanford S.: Dependence of ozone production on NO and hydrocarbons in the troposphere, Geophys. Res. Lett., 24, 2299–2302, 1997.

Leighton, P. A.: Photochemistry of Air Pollution, Academic, San Diego, Calif., 1961.

McFarland, M., Kley, D., and Drummond, J. W.: Simultaneous NO, NO_2, and O_3 vertical profile measurements from ground level to 6 km, paper presented at the 4th Biennial Rocky Mountain Regional Meeting, Am. Chem. Soc., Boulder, Colo., June 1978.

Mihelcic, D., Holland, F., Hofzumahaus, A., Hoppe, L., Konrad, S., Musgen, P., Patz, H. W., Schafer, H. J., Schmitz, T., Volz-Thomas, A., Bachmann, K., Schlomski, S., Platt, U., Geyer, A., Alicke, B., and Moortgat, G. K.: Peroxy radicals during BERLIOZ at Pabstthum: Measurements, radical budgets and ozone production, J. Geophys. Res., 108, 8254–8268, doi:10.1029/2001JD001014, 2003.

Milford, J., Gao, D., Sillman, S., Blossey, P., and Russell, A. G.: Total reactive nitrogen (NO_y) as an indicator for the sensitivity of ozone to NO_x and hydrocarbons, J. Geophys. Res., 99,

3533–3542, 1994.
Monks, P. S., Carpenter, L. J., Penkett, S. A., Ayers, G. P., Gillett, R. W., Galbally, I. E., and Meyer, C. P.: Fundamental ozone photochemistry in the remote boundary layer: The SOAPEX experiment, measurement and theory, Atmos. Environ., 32, 3647–3664, 1998.
Monks, P. S.: A review of the observations and origins of the spring ozone maximum, Atmos. Environ., 34, 3545–3561, 2000.
Paulson, S. E. and Orlando, J. J.: The reactions of ozone with alkenes: An important source of HO_x in the boundary layer, Geophys. Res. Lett., 23, 3727–3730, 1996.
Parrish, D. D., Trainer, M., Williams, E . J., Fahey, D. W., Hubler, G., Eubank, C. S., Liu, S. C., Murphy, P. C., Albritton, D. L., and Fehsenfeld, F.: Measurements of the NO-O_3 photostationary state at Niwot Ridge, Colorado, J. Geophys. Res., 91, 5361–5370, 1986.
Platt, U.: The origin of nitrous and nitric acid in the atmosphere, in: Chemistry of Mutltiphase Atmospheric System, edited by: Jäschke, W., 299–319, Spring-Verlag, New York, 1986.
Qi, B., Kanaya, Y., Takami, A., Hatakeyama, S., Kato, S., Sadanaga, Y., Tanimoto, H., and Kajii, Y.: Diurnal peroxy radical chemistry at a remote coastal site over the sea of Japan, J. Geophys. Res., 112, D17306, doi:10.1029/2006JD008236, 2007.
Ren, X. R., Brune, W. H., Canterll, C. A., Edwards, G. D., Shirley, T., Metcalf, A. R., Trainer, M. E., Hsie, Y., McKeen, S. A., Tallamraju, R., Parrish, D. D., Fehsenfeld, F. C., and Liu, S. C.: Impact of natural hydrocarbons in hydroxyl and peroxy radicals at a remote site, J. Geophys. Res., 92, 11879–11894, 1987.
Ritter, J. A., Stedman, D. H., and Kelly, T. J.: Ground-level measurements of nitric oxide, nitrogen dioxide and ozone in rural air, in: Nitrogenous Air Pollutants: Chemical and Biological Implications, edited by: Grosjean, D., Butterworth, Stoneham, Mass., 1979.
Robert, L. L.: Hydroxyl and Peroxy Radical Chemistry in a Rural Area of Central Pennsylvania: Observations and Model Comparisons, J. Atmos. Chem., 52, 231–57, 2005.
Salisbury, G., Monks, P. S., Bauguitte, S., Bandy, B. J., and Penkett, S. A.: A seasonal comparison of the ozone photochemistry in clean and polluted air masses at Mace Head, Ireland, J. Atmos. Chem., 41, 163–187, 2002.
Sander, S. P., Friedl, R. R., Golden, D. M., Kurylo, M. J., Huie, R. E., Orkin, V. L., Ravishankara, A. R., Kold, C. E., and Molina, M. J.: Chemical kinetics and photochemical data for use in stratospheric modeling, evaluation number 14, JPL Publication 02-25, NASA Jet Propulsion Laboratory, Pasadena, California, 2003.
Stockwell, W. R., Kirchner, F., Kuhn, M., and Seefeld, S.: A new mechanism for regional atmo-

spheric chemistry modeling, J. Geophys. Res., 102, 25847–25879, 1997.
Tanimoto, H., Kajii, Y., Hirokawa, J., Akimoto, H., and Minko, N. P.: The atmospheric impact of boreal forest fires in far eastern Siberia on the seasonal variation of carbon monoxide: Observations at Rishiri, a northern remote island in Japan, Geophys. Res. Lett., 27, 4073–4076, 2000.
Tonnesen, G. S. and Dennis, R. L.: Analysis of radical propagation efficiency to assess ozone sensitivity to hydrocarbons and NO_x: 1. Local indicators of instantaneous odd oxygen production sensitivity, J. Geophys. Res., 105, 9213–9225, 2000.
WMO, World Meteorological Organization: Scientific Assessment of Ozone Depletion: 1998, in: Global Ozone Research and Monitoring Project Report, Rep. 44, Geneva, ISBN: 92-807-1722-7, 1999.

ACPD
10, 10551–10587, 2010

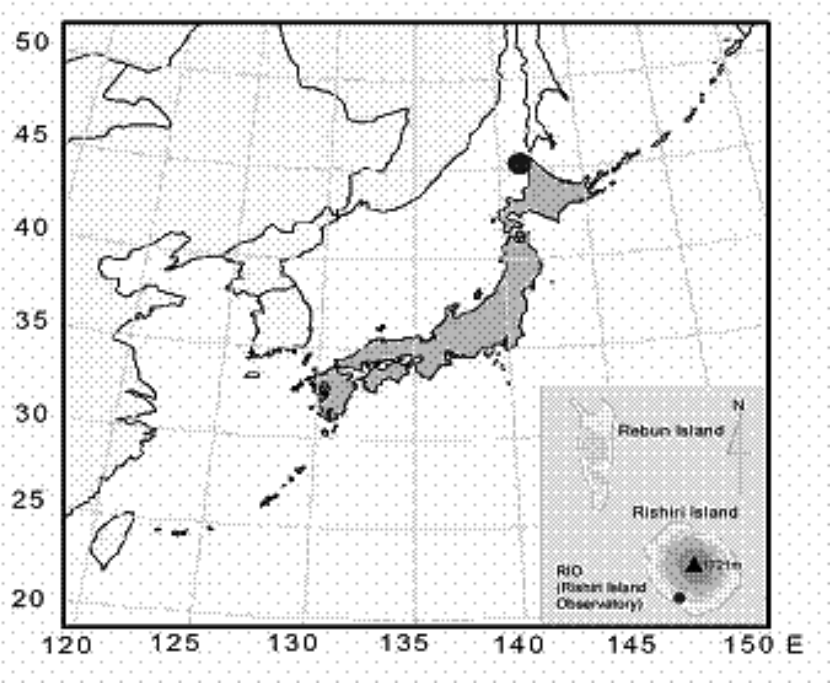

Fig. 1. Geographical location of Rishiri island and Rishiri Island Observatory.

ACPD

10, 10551–10587, 2010

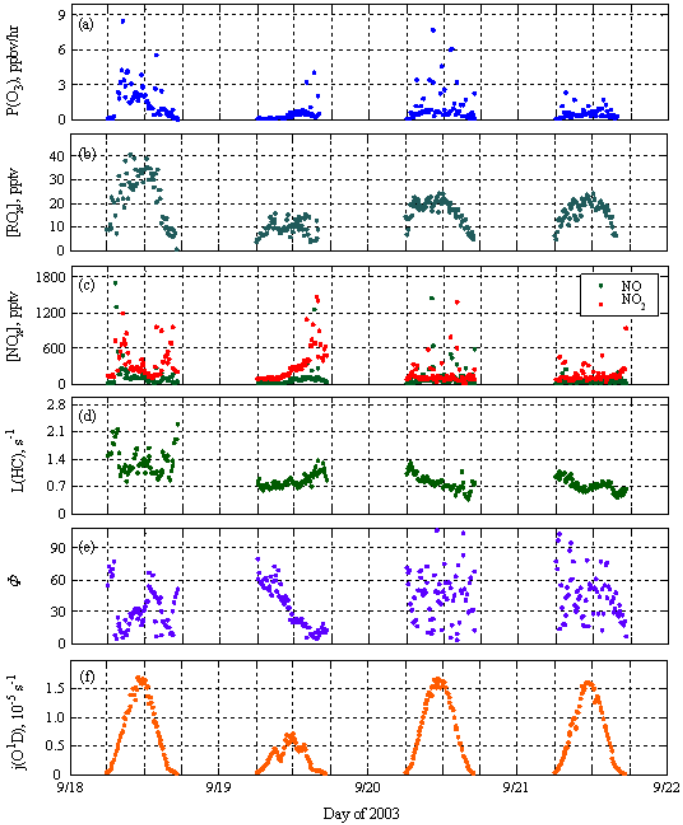

Fig. 2. Time series of **(a)** ozone production rate ($P(O_3)$), **(b)** RO_x, **(c)** NO_x (NO and NO_2), **(d)** OH reactivity due to HC (L(HC)), (e) Φ and **(f)** $j(O^1D)$ in 10-min averages during 18–21 September, 2003.

ACPD
10, 10551–10587, 2010

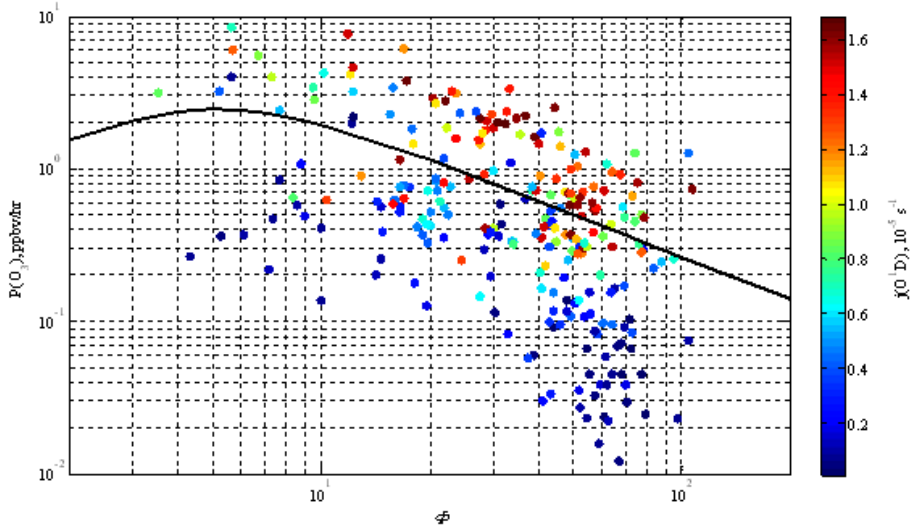

Fig. 3. Dependence of $P(O_3)$ on the indicator Φ for daytime 10-min averaged data on 18–21 September 2003. The color of the dots shows the values of $j(O^1D)$. The black curve shows the modeled trend of $P(O_3)$ with increasing Φ at 11:50 JST on 18 September 2003.

ACPD
10, 10551–10587, 2010

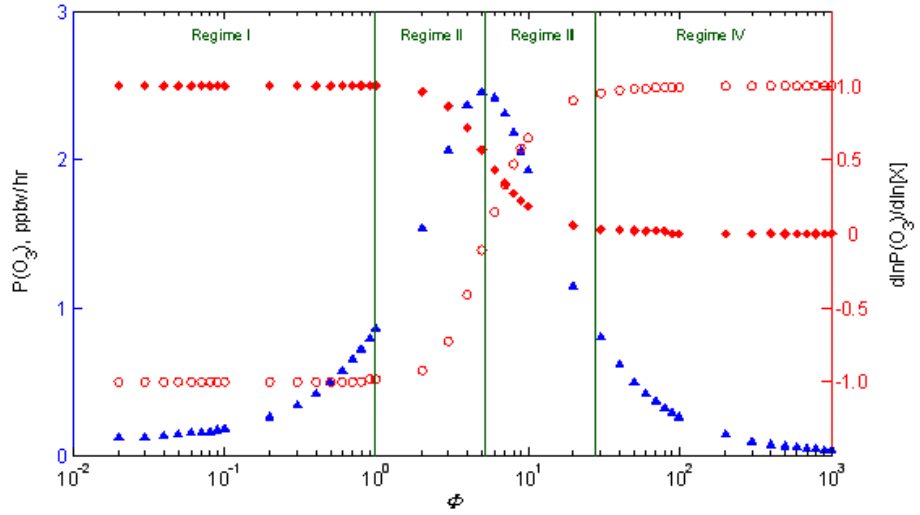

Fig. 4. Dependence of **(a)** $d\ln P(O_3)/d\ln[NO]$ (shown by open circle), $d\ln P(O_3)/d\ln[HC]$ (shown by square) and $P(O_3)$ (shown by triangle) on Φ at 11:50 JST on 18 September 2003.

ACPD
10, 10551–10587, 2010

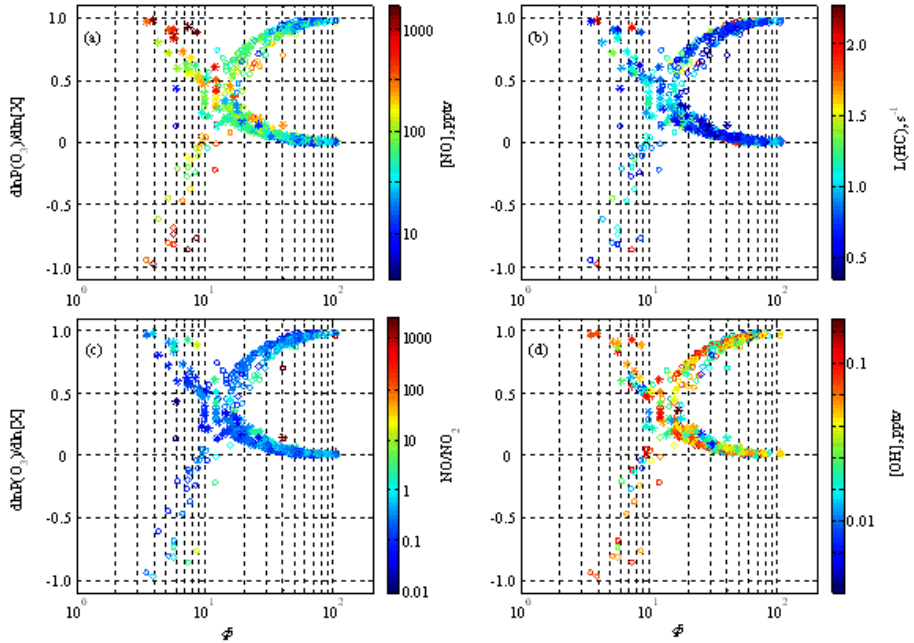

Fig. 5. Dependence of $d\ln P(O_3)/d\ln[NO]$ (shown by open circle) and $d\ln P(O_3)/d\ln[HC]$ (shown by asterisk) on Φ for daytime 10-min averaged data on 18–21 September 2003. The color shows **(a)** the mixing ratio of NO, **(b)** the value of the OH reactivity due to HC, **(c)** the NO/NO_2 ratio and **(d)** observed OH concentration on the corresponding time.

ACPD
10, 10551–10587, 2010

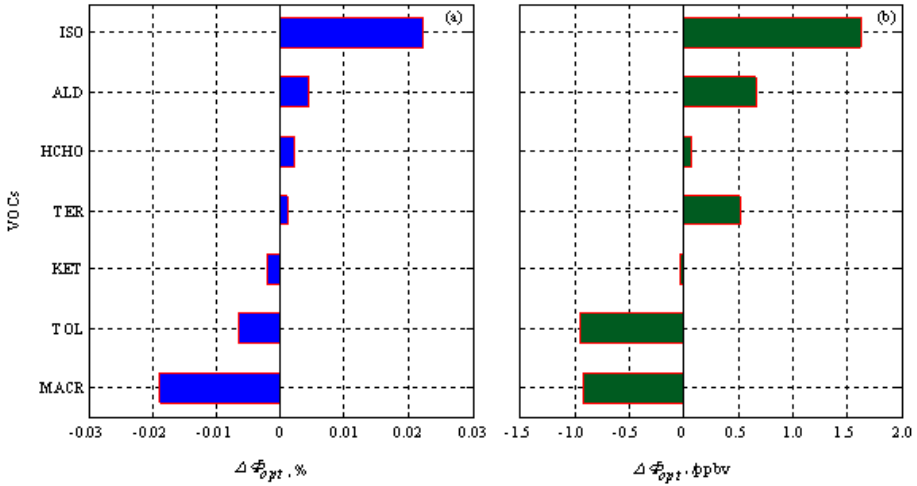

Fig. 6. Compare of the Φ_{opt} change ($\Delta\Phi_{opt}$) due to the increase of the VOCs concentration at 11:50 JST on 18 September. TER: monoterpenes.

ACPD
10, 10551–10587, 2010

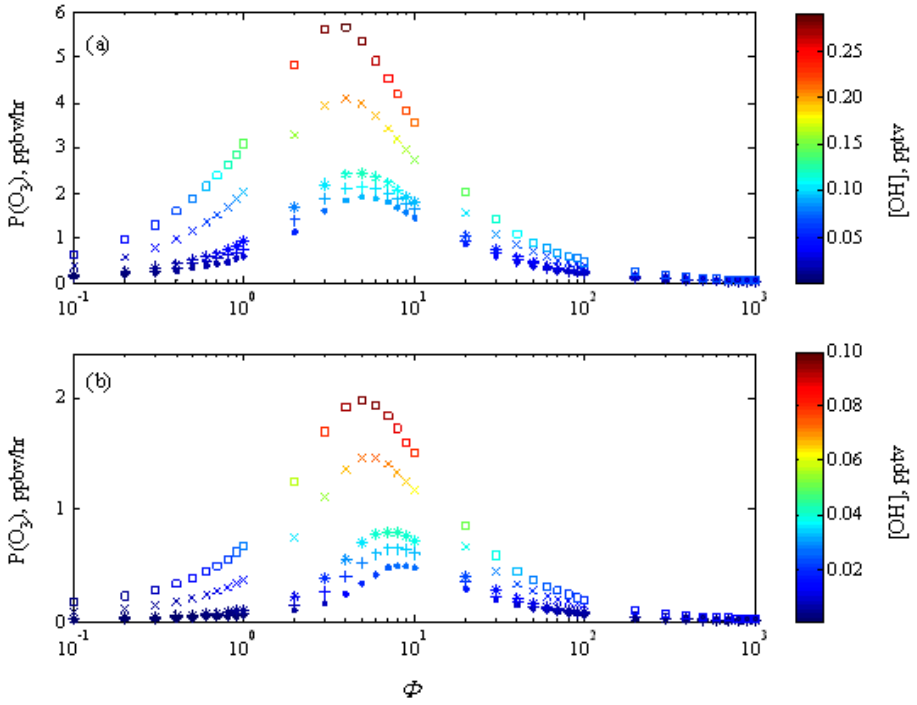

Fig. 7. Dependence of $P(O_3)$ on Φ when the concentration of O_3 is constrained to 1 ppbv (shown by point), 5 ppbv (shown by plus sign), 10 ppbv (shown by asterisk), 50 ppbv (shown by cross) and 100 ppbv (shown by square), respectively. The photolysis rate is constrained to it observed on **(a)** 11:50 JST 18 September, and **(b)** 06:00 JST 18 September. The NO/NO_2 ratio and other conditions are constrained to those observed on 11:50 JST 18 September. The color of the dots shows the mixing ratio of OH radical.

ACPD
10, 10551–10587, 2010

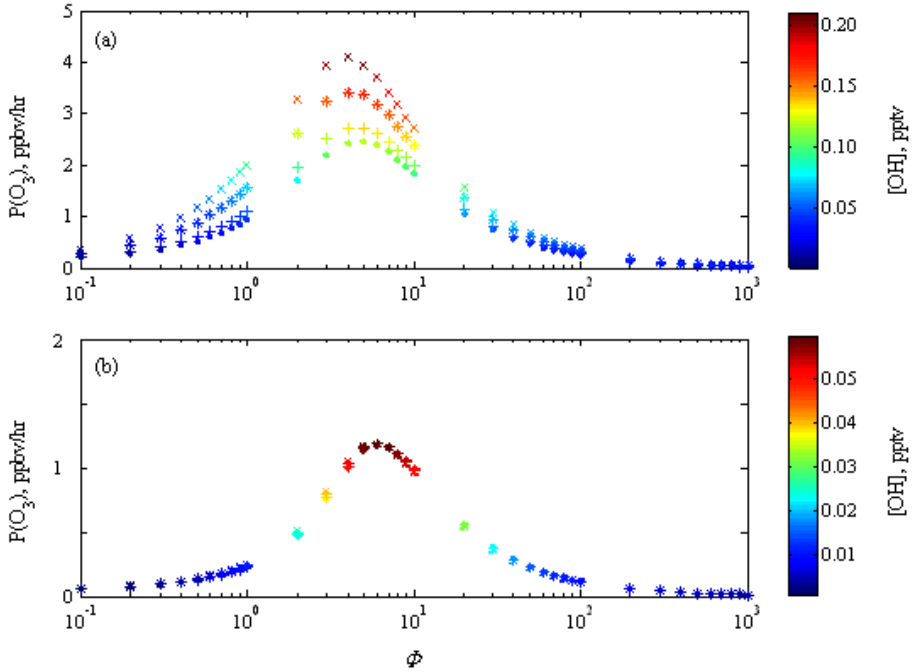

Fig. 8. Dependence of $P(O_3)$ on Φ when the relative humidity is constrained to 10% (shown by point), 20% (shown by plus sign), 50% (shown by asterisk) and 90% (shown by cross) respectively. The photolysis rate is constrained to it observed on **(a)** 11:50 JST 18 September, and **(b)** 06:00 JST 18 September. The NO/NO_2 ratio and other conditions are constrained to those observed on 11:50 JST 18 September. The color of the dots shows the mixing ratio of OH radical.

ACPD
10, 10551–10587, 2010

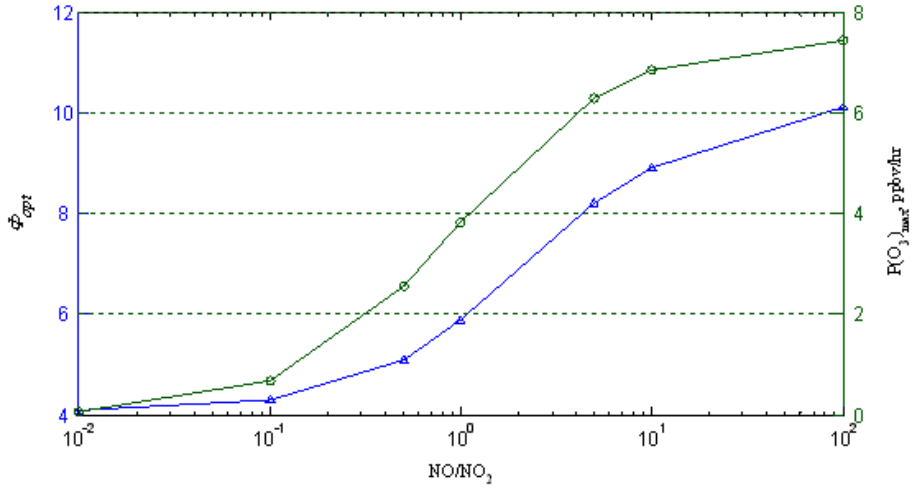

Fig. 9. Dependence of Φ_{opt}, the maximum $P(O_3)$ ($P(O_3)_{max}$)on different NO/NO_2 ratio.

ACPD

10, 10551–10587, 2010

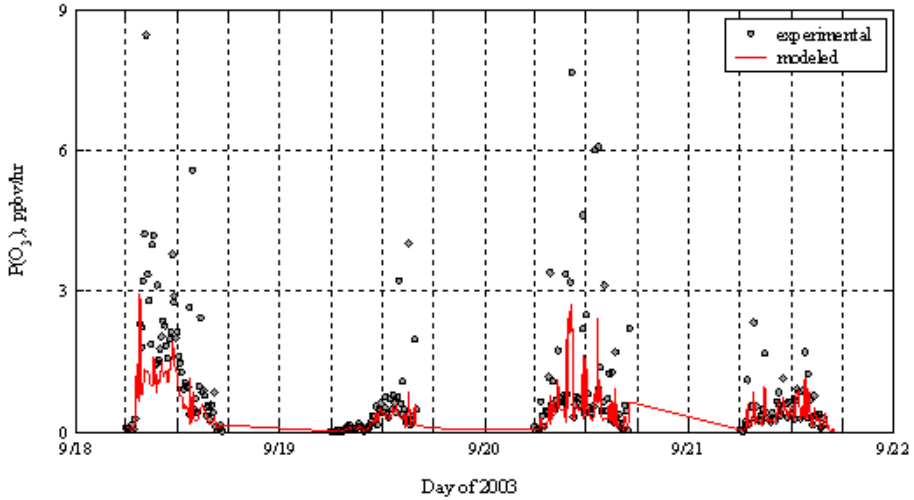

Fig. 10. Time series of experimental and modeled $P(O_3)$ in 10-min averages during 18–21 September, 2003.

ACPD
10, 10551–10587, 2010

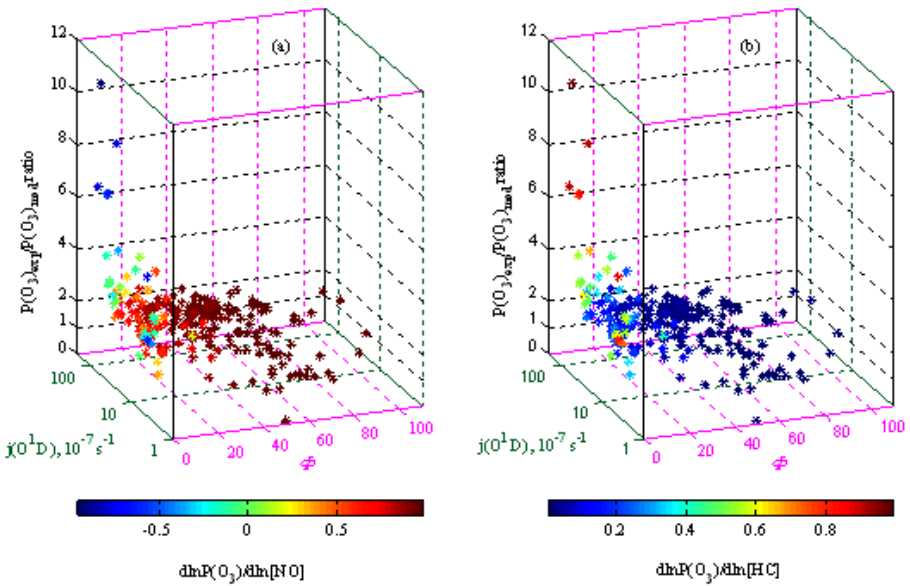

Fig. 11. Dependence of the experimental $P(O_3)$ to modeled $P(O_3)$ rate ($P(O_3)_{exp}/P(O_3)_{mod}$) on **(a)** $d\ln P(O_3)/d\ln[NO]$ and **(b)** $d\ln P(O_3)/d\ln[HC]$ at different $j(O^1D)$ and Φ values for daytime 10-min averaged data on 18–21 September 2003. The color of the asterisks shows (a) $d\ln P(O_3)/d\ln[NO]$ and (b) $d\ln P(O_3)/d\ln[HC]$ on the corresponding time.

ACPD
10, 10551–10587, 2010

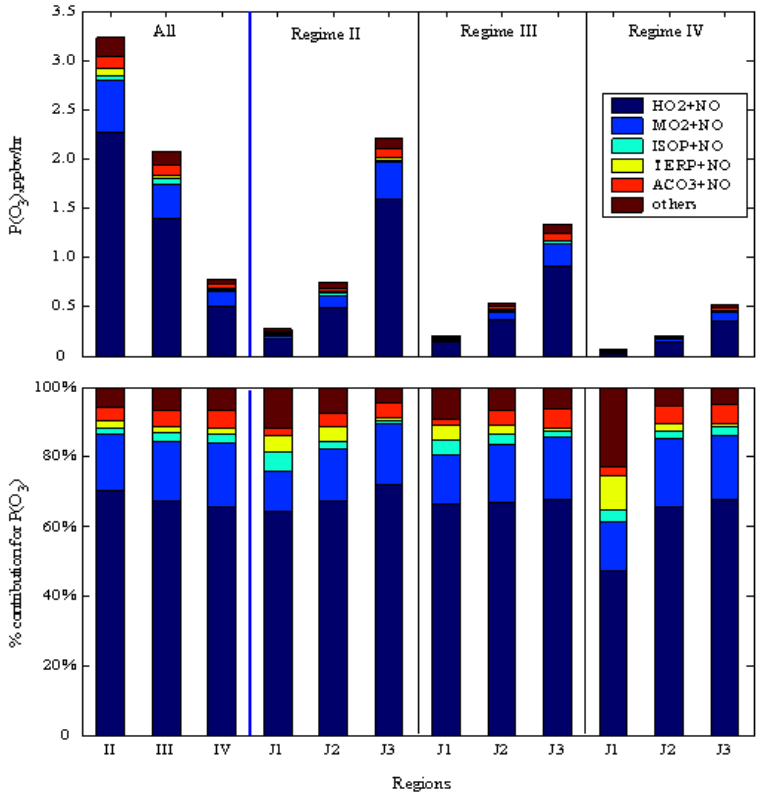

Fig. 12. Itemization of $P(O_3)$ calculated for different Regimes: **(a)** Regime II, **(b)** Regime III, and **(c)** Regime IV. The 10-min average $P(O_3)$ data are categorized into 3 classes by $j(O^1D)$ (s^{-1}) values: (J1) $j(O^1D)<10^{-6}\,s^{-1}$, (J2) $10^{-5}\,s^{-1} > j(O^1D)>10^{-6}\,s^{-1}$, and (J3) $j(O^1D)>10^{-5}\,s^{-1}$. TERP: peroxy radicals form monoterpenes.

ACPD
10, 10551–10587, 2010

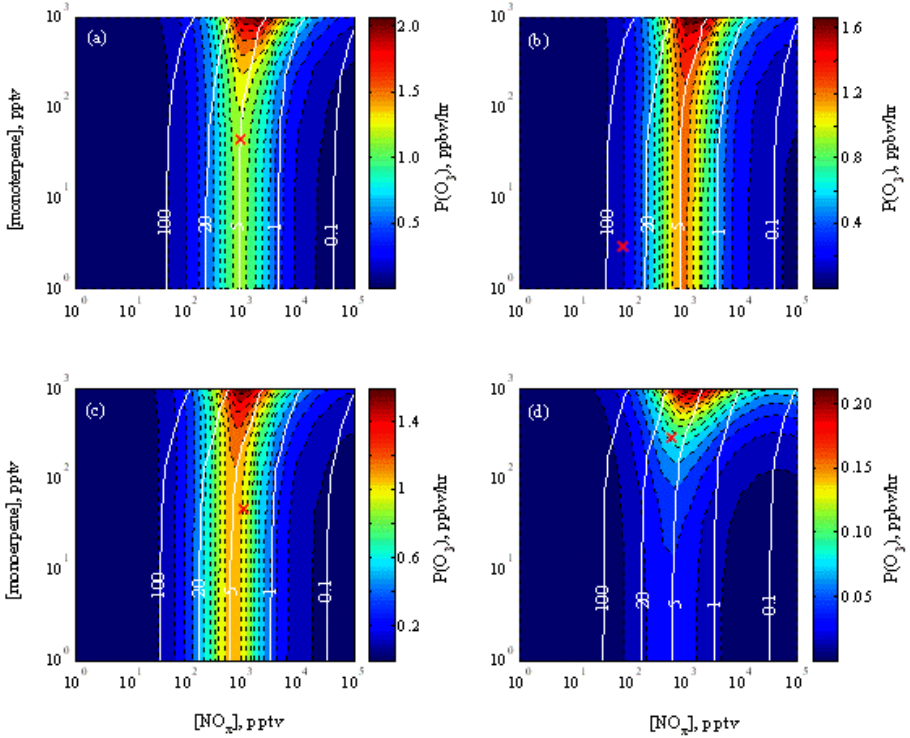

Fig. 13. Calculated dependence of $P(O_3)$ upon monoterpenes concentrations and NO_x concentrations. Other conditions including $j(O^1D)$ were constrained to those observed on the selected time: **(a)** 08:40 JST 18 September, **(b)** 13:10 JST 21 September, **(c)** 13:00 JST 20 September, and **(d)** 06:40 JST 21 September. The contour plots of Φ are shown by whiter lines. Red crosses indicated the observed concentrations of monoterpenes and NO_x on the selected time.

ACPD
10, 10551–10587, 2010